Melt Index Prediction by RBF Neural Network with an ICO-VSA Hybrid Optimization Algorithm

Mingyu Huang, Xinggao Liu, Jiubao Li

State Key Laboratory of Industrial Control Technology, Department of Control Science and Engineering, Zhejiang University, Hangzhou 310027, People's Republic of China

Received 7 May 2011; accepted 12 January 2012
DOI 10.1002/app.36814
Published online in Wiley Online Library (wileyonlinelibrary.com).

ABSTRACT: Melt index (MI) is considered as one of the most significant parameter to determine the quality and the grade of the practical polypropylene polymerization products. A novel ICO-VSA-RNN (RBF neural network with ICO-VSA algorithm) MI prediction model is proposed based on radial basis function (RBF) neural network and improved chaos optimization (ICO), and variable-scale analysis (VSA), where the ICO is first added and then combined with the VSA to overcome the defects of ICO and VSA, then the parameters of the RBF neural network are optimized with them. At last, the RBF neural network model for MI prediction model is developed. Further researches on the optimal RBF neural network model of MI prediction are carried out with the data from a real industrial plant, and the prediction results show that the performance of this prediction model is much better than the RBF neural network model without optimization. © 2012 Wiley Periodicals, Inc. J Appl Polym Sci 000: 000–000, 2012

Key words: polypropylene; radial basis function network; ICO and VSA; melt index prediction

INTRODUCTION

Polypropylene is a thermoplastic resin obtained by the polymerization of propylene, is the most important downstream product of propylene, 50% of the propylene in the world are used to make polypropylene,[1] and it is one of the five general-purpose plastic which is closely related to our daily life. Because polypropylene products have a wide range of uses, polypropylene industry has become a big business which has the great influences to the world in aspects of industry, economy, military, and so on. MI, which determines the difference uses of the products, is the most significant parameter to control the quality of the polypropylene products. The traditional measurement method used is the off-line analysis in the laboratory. However, this off-line analysis method will bring 2–4 h^2 of time delay, which results in the lost of the possibility of the real-time control. Therefore, a MI on-line analysis model, which can predict the MI in time, will be useful.

Since a MI online analysis model can be constructed with the process of the polypropylene, it is certainly that there are some relationships between the MI and other easy-measured variables. The MI prediction model constructed with the process of the polypropylene can use the chemical and physical relationships to predict the difficult-measured variables from the easy-measured variables. However, developing the model by the process of the industrial process mechanism[3–8] is faced a huge challenge, due to the complexity from the kinetic behavior, the engineering activity, and the operation of polymer plants.

On the other hand, some plants have already used the statistical methodologies to provide information for process design, control, and monitoring.[9,10] At the same time, neural network has been widely applied to build the prediction model because of their good performance in the field of the adaptive capabilities to nonlinear behaviors. Han[11] used three methods, which are partial least squares (PLS), support vector machines (SVM), and artificial neural networks in polymerization process. Kong and Yang[12] added the principal component analysis (PCA) and PLS to the RBF network to develop a model for MI prediction of the PP process. Li and Liu add the particle swarm optimization, simulated

Correspondence to: X. Liu (liuxg@iipc.zju.edu.cn).
Contract grant sponsor: Joint Funds of NSFC-CNPC of China; contract grant number: U1162130.
Contract grant sponsor: National High Technology Research and Development Program (863); contract grant number: 2006AA05Z226.
Contract grant sponsor: International Cooperation and Exchange Project of Science and Technology Department of Zhejiang Province; contract grant number: 2009C34008.
Contract grant sponsor: Zhejiang Provincial Natural Science Foundation for Distinguished Young Scientists; contract grant number: R4100133.

© 2012 Wiley Periodicals, Inc.

annealing (PSO-SA).[13] Shi and Liu[14,15] and Shi[16] also developed several soft-sensor models for MI prediction based on independent component analysis, multi-scale analysis and RBF neural network (ICA-MSA-RBF), MSA-PCA-RBF and least squares, support vector machines (LS-SVM), and so on. As the neural network developed with these methods, quite a good performance in the prediction of the PP polymerization process is obtained. Although these works have provided good predictions, much better performance and university generation of the model are still the most important targets in academic and industry.

In this article, the most significant work is to find out the relationships between the difficult-measured variables and the easy-measured variables. First the RBF neural network is trained based on several pairs of target-input data, so the RBF neural network can predict the MI value from the new values of the input variables that are unseen in training. Then, the prediction model will be developed. The adaptive capability in response to nonlinear relationship of the neural network is the key that determines the network's prediction accuracy. The key to determine the RBF neural network's adaptive capability is its parameters, such as weight, centers, bias, etc.[17] A general set of the parameters cannot always ensure the model to have a high prediction accuracy for the PP process. Therefore, an optimization of the network's parameters is necessary to improve the accuracy of the MI prediction. So far, many intelligent algorithms have been mentioned, such as PCA, PLS, SVM, CO (Chaos Optimization), VSA, and so on, which have their advantages and disadvantages, respectively. Here CO and VSA have been used to optimize the parameters of the RBF neural network. Compared with the algorithms mentioned above, CO and VSA have some outstanding characteristics and they can search more efficiently, narrow the search space and optimize the variables to improve search precision. However, the traditional CO and the traditional VSA have inherent defects. For the former, in some situations it will fall into a local optimum. If an optimization factor is added to CO, it will search much more efficiently, which produces an ICO algorithm. For the latter, it can reduce the range of the search, but this optimization performance depends on the initial solutions. Therefor a novel hybrid algorithm, where the ICO is firstly added and then combined with VSA, is presented. The new hybrid algorithm will overcome the defects of both the traditional CO and VSA, and achieves a perfect optimizing performance. At last this new algorithm is used to optimize the parameters of the network, and the best parameters of the RBF neural network are obtained.

How to add the intelligent optimizing algorithms to optimize the parameters of the RBF neural network and then use the network to predict the MI of the PP process is a project with great deal of research significances. Here, a novel MI prediction model, ICO-VSA-RNN model, is obtained, and the results below will discuss and conclude details about this model.

RBF NEURAL NETWORK AND NOVEL ICO-VSA HYBRID ALGORITHM

RBF neural network

The RBF neural network has been widely used for the quality prediction of the complex and correlated PP process.[18–21] It's a feed-forward network consists of three layers: the input layer, the hidden layer, and the output layer. The input layers deal with the input vector x. The role of the hidden layer is to complete the input of the nonlinear transformation. Output layers are used to complete a linear combination of hidden layer output. The RBF neural network can be described in Euclidean space: $T : R^r \rightarrow R^s$. Let $x^p \in R^r$ be the input vector and $c^i \in R^r (i = 1, 2, ..., k)$ be the center. The result of output is formed by a linear combination of the hidden layer's output, that is

$$y_k(x_p) = \sum_{i=1}^{N} w_{ki} \Phi_i(||x_p - c_i||), \quad i = 1, 2, ..., M \qquad (1)$$

where $||\cdot||$ is the Euclidean distance, N is the number of the hidden layer nodes, $\Phi_i(\cdot)$ is the result of the hidden layer node, w_{ki} is the output weight, x_p is the input vector, y_k is the output of its corresponding output node, M is the number of the output nodes. And the hidden layer nodes use the Gaussian activation function to get the result,

$$\Phi_i(||x_p - c_i||) = -\exp\left(-\frac{(||x_p - c_i||)^2}{2\sigma_j}\right), \quad i = 1, 2, ..., M \qquad (2)$$

where c_i and σ_i are the center and the width of its corresponding node in the hidden layer, respectively. They can control the speed of decay of the Gaussian function, that is, control the response of the hidden layer neurons to the range of the input.

Novel ICO-VSA algorithm

Basic CO algorithm

The basic idea of CO algorithm is to introduce the chaotic state into the variables. Because the CO algorithm has got ergodicity, randomness and other characteristics, which makes it to searches more efficient.[22,23]

The CO is an iterative algorithm. First it is needed to define the number of iteration steps k and then

different variables x_i should be initialized with small difference to get different chaotic variables f_i [generally random values of the range of (0,1)].

The second step is to use the method of carrier to introduce the chaos variables into the optimization variable, that is

$$x_i' = c_i + d_i x_i \tag{3}$$

Comparing the corresponding target value $f_i(k)$ of the new chaos variable $x_i(k)$, and save the better variable and its corresponding target value and number of iteration steps plus one,

$$\text{If} \quad f_i(k) \le f, \quad x_i = x_i(k) \quad f = f(k) \tag{4}$$

And then return to the second step. After achieving the maximum number of iteration steps, stop the process of iteration stopped and output the best variables x_i and its corresponding target value f, respectively.

Variable-scale analysis

VSA is a stochastic gradient method to obtain the optimum solutions for many optimization problems.[24–26] VSA method use the characteristics of chaos to map the chaos variables to the region of the optimization variables, continued to narrow the search space and optimize the variables to improve search precision, and thus has a higher search efficiency. The method is shown blow:

Step 1: Calculate the parameters, that is

$$a_{i+1} = x_i - \gamma \cdot (b_i - a_i) \tag{5}$$

$$b_{i+1} = x_i + \gamma \cdot (b_i - a_i) \tag{6}$$

To make that the new range does not go out of the range:

$$\text{If} \quad a_{i+1} < a_i, \quad a_{i+1} = a_i \tag{7}$$

$$\text{If} \quad b_{i+1} > b_i, \quad b_{i-1} = a_i \tag{8}$$

where $\gamma \in (0, 0.5), x_i$ is the best variable.

Step 2: Transform the variables, that is

$$x_i^* = \frac{x_i - a_{i+1}}{b_{i+1} - a_{i-1}} \tag{9}$$

After these steps, the search space will be reduced and the model will have the high search efficiency.

ICO-VSA hybrid algorithm

Although the CO has many characteristics which can makes it to searches more efficiently, after some generations the speed of ergodicity is slow and easily falling into a local optimum.[27,28] To improve the search efficiency, the optimization factors have been added to CO algorithm. This ICO algorithm has a good performance to improve the search efficiency. The VSA algorithm has great ability to narrow the space and then to find out the optimum solution quickly around the initial state. But a difficult problem is that it is hard to find out the appropriate initial state near the optimum. So it is also hard for the VSA to obtain the optimum.

The ICO-VSA hybrid algorithm is a combination of ICO, VSA, and RNN, but modifying the RNN first. The first step is use the RNN to build a basic model and then use the ICO-VSA algorithm to optimize the parameters of the RNN. The procedures of ICO-VSA-RNN model are shown as follows:

Step 1: Create a basic RNN and then initialize the input vectors and the target vectors. After determining the mean squared error goal, spread of the radial basis function, the maximum number of neurons and the number of neurons to add between displays, and returns a basic RNN.

Step 2: Use the ICO algorithm to optimize the parameters of the RNN:

Step 2.1: Initializes the sequence number of iteration: $k = 0$, the maximal sequence number of iteration: $N = 100$, the minimal error of the output predicted by the RNN and the real output: min_err $= 1$, and define a random constant: $m \in (0, 1)$, and define constants $i = a = 1$;

Step 2.2: Uses input vectors to train the RNN and then calculate the sum of square root of the error (err) between the output predicted by the RNN and the real output. If err<min_err, then set the parameters of this RNN as the best parameter (best_w) and use these best parameters to define the RNN next time.

Step 2.3: Performs the ICO algorithm to find out the appropriate initial state near the optimum:

$$t = 4 * M * (1 - m) \tag{10}$$

$$m = \text{mod}(2 * t, 1) \tag{11}$$

$$\text{If} \quad k > 1, \quad t = \left(1 - \frac{0.49}{i - 1}\right) * m \quad m = t \tag{12}$$

$$w = \text{best}_\text{w} + a. * \text{best\_}w. * (0.5 - m) \tag{13}$$

where t and m are used as the optimization factors, w and best_w are the parameters of the RNN and the best parameters, respectively. Equation (12) is the logistic function and eq. (13) is the tent function, both two functions all have good performance in the Chaos optimization.[29–33]

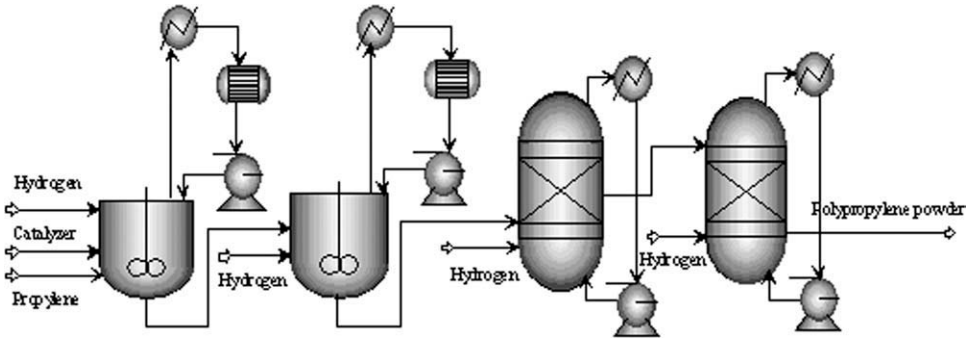

Figure 1 General scheme of propylene polymerization.

Step 2.4: Let $k = k + 1$ and set the parameters got from the eq. (13) as the new parameters of the RNN. If $k < N$, go to step 2.2; else go to step 3.1.

Step 3: Performs the VSA algorithm to narrow the search space and to improve the search efficiency.

Step 3.1: Initializes the sequence number of the iteration: $k = 0$, $a = a - a/100$ and $i = 0$.

Step 3.2: If $a > 1/100$, go to step 2.3; else output the best parameters (best_w), and considered them as the parameters of the RNN model which is used to predict melt index.

CASE STUDY

The apparent consumption of China's polypropylene industry will still maintain a high growth rate in next few years, and polypropylene industry in China will have a bright future. A propylene polymerization process is considered in this article, and Figure 1 shows the schematic diagram of the process. The process consists of four reactors in series, the first two continuous stirred-tank reactors (CSTR) are liquid phase reactors, and the latter two are fluidized-bed reactors (FBR).The polymerization mainly reacts in the first two reactors in a liquid phase, and in the latter two reactors the reactions are completed in vapor phase. Melt index, is a thermoplastic in a certain temperature and pressure (230°C ± 0.4°C, 2.16 ± 0.01 kg), the quality of the melt flow through the standard aperture (diameter 2.0950 ± 0.0005 mm, Length 8.00 ± 0.02 mm) within 10 min. The greater the value of MI is, the smaller the molecular weight of powder is, so the melt index reflects the size of the product molecular weight. MI is an important part of quality control of a propylene polymerization process, which determines different brands of products and different grades of product quality.

To develop a prediction model to estimate the MI should care about many variables should be considered. According to the actual production process and process analysis, the main operating variables are nine easy measurable variables: the flow rate of three streams of propylene into the reactors (f_1, f_2, f_3), the flow rate of main catalyst and aid-catalyst (f_4, f_5), reactor temperature (T), pressure (p), liquid level (l), percentage of hydrogen in vapor phase (a). To avoid the happening of the abnormal situations happen and to improve the quality of the prediction model a great number of operational data has been taken from the DCS historical recorded in the real plant and are filtered first, and these are operational data points of polypropylene products of brand F401. And then normalization is also used to the input and output variables with respect of the maximum and minimum values. Table IV shows the operational dataset points used in the training of the model. Because the data taken from the real plant are not the most suitable training dataset, how to choose the suitable dataset is also an important procedure. The

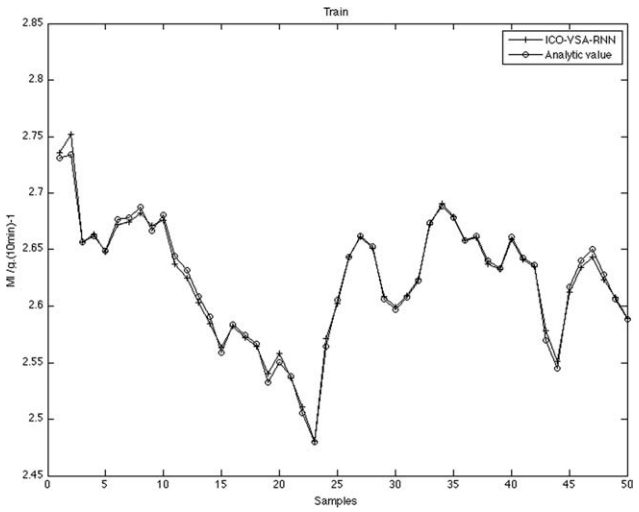

Figure 2 Training results of ICO-VA-RNN model.

TABLE I
Performance of the ICO-VSA-RNN and RNN on the Testing Dataset

Model	MAE	MRE (%)	RMSE	TIC
RNN	0.0293	1.12	0.0409	0.0078
ICO-VSA-RNN	0.0078	0.30	0.0086	0.0016

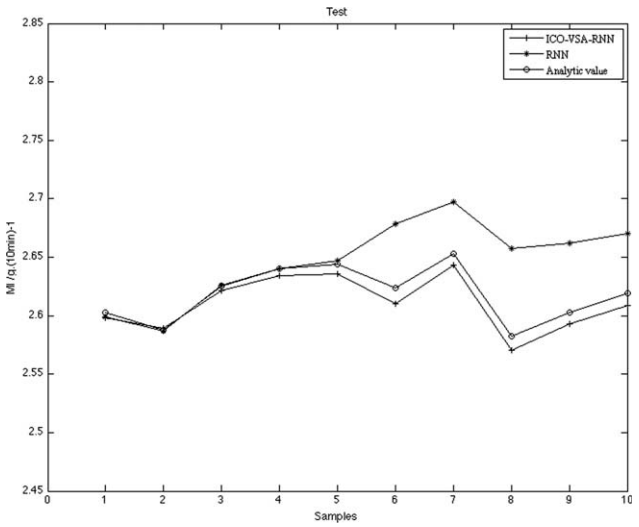

Figure 3 Performance of the ICO-VA-RNN and RNN on the testing dataset.

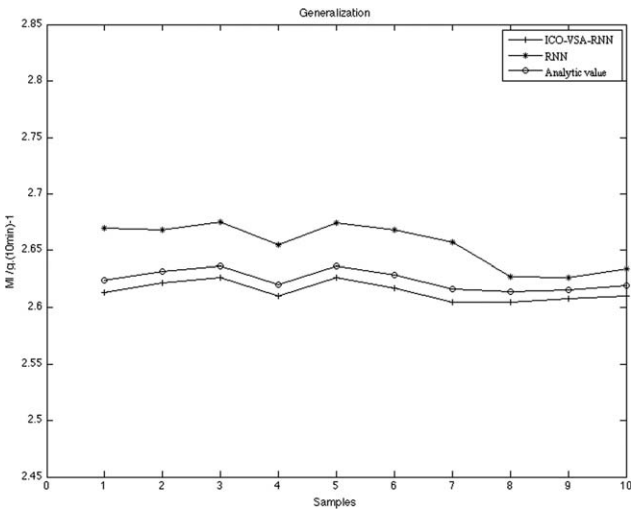

Figure 4 Performance of the ICO-VA-RNN and RNN on the generalization dataset.

average residence time for this real propylene polymerization process is about 2 h, which has been considered in the data initialization. The method to construct the training dataset here is dividing the data into training dataset, testing dataset, and generalization dataset to the series of the recorded data. After that an adaptive neural network model are developed based on the training dataset. After the neural network model is built, the testing dataset and the generalization dataset are used to test the accuracy and the university of the model's prediction respectively. There are 50 points in the training dataset and 10 points in the testing dataset, the other 10 points is left to the generalization dataset. The training and testing dataset are taken from the same batch, whereas the generalization dataset are taken from the other batch. This is significant to be noted, because on this situation the prediction on the testing and generalization dataset is believable. The RNN used in this article has four neurons and the ICO-VSA is used to training its weight, bias, and so on. To study the quality of the MI prediction, many different ways are used to represent the difference between the output of the model and the desired output (the offline analytic MI values from laboratory). In this article, the following measures are used for model evaluations: mean absolute error (MAE), mean relative error (MRE), root of mean square error (RMSE), and Theil's inequality coefficient (TIC). The error indicators are defined as following:

$$\mathrm{MAE} = \frac{1}{N}\sum_{i=1}^{N}|y_i - \hat{y}_i| \tag{14}$$

$$\mathrm{MRE} = \frac{1}{N}\sum_{i=1}^{N}\left|\frac{y_i - \hat{y}_i}{y_i}\right| \tag{15}$$

$$\mathrm{RMSE} = \sqrt{\frac{1}{N}\sum_{i=1}^{N}(y_i - \hat{y}_i)^2} \tag{16}$$

$$\mathrm{TIC} = \frac{\sqrt{\sum_{i=1}^{N}(y_i - \hat{y}_i)^2}}{\sqrt{\sum_{i=1}^{N} y_i^2} + \sqrt{\sum_{i=1}^{N} \hat{y}_i^2}} \tag{17}$$

where y_i and $\hat{y}_i$ denote the measured value and predicted result of MI respectively.

The MAE, MRE, and RMSE confirm the prediction accuracy of the proposed methods. TIC indicates a good level of agreement between the proposed model and the studied process.[34]

Figure 1 shows the general scheme of propylene polymerization and almost 55% of the propylene polymerization uses this scheme in the world.

The training results are shown in Figure 2, where the curve marked with crosses is the MI value

TABLE II
Performance of the ICO-VSA-RNN and RNN on the Generalization Dataset

Model	MAE	MRE (%)	RMSE	TIC
RNN	0.0311	1.18	0.0334	0.0063
ICO-VSA-RNN	0.0101	0.39	0.0102	0.0019

TABLE III
Reported Best Results in MI Prediction and Comparison Between Them and This Study

Work	MAE	MRE (%)	RMSE	TIC
Shi and Liu[14]	0.0663	2.72	–	–
Shi and Liu[15]	0.0218	0.83	0.0287	0.0055
Li and Liu[13]	0.0635	2.49	0.0312	0.0138
This study	0.0078	0.30	0.0086	0.0016

TABLE IV
The Operational Dataset Points used in the Model's Training

	a	f_4	f_5	f_1	f_2	f_3	l	p	T
1	0.8628	0.3682	0.6584	0.9	0.1873	0.8904	0.8959	0.9	0.5615
2	0.9	0.1711	0.6554	0.8893	0.1	0.8973	0.9	0.7617	0.4846
3	0.6054	0.3154	0.6638	0.8652	0.2455	0.8938	0.8935	0.6553	0.4692
4	0.6302	0.2821	0.6652	0.7714	0.3545	0.8938	0.887	0.683	0.5615
5	0.5868	0.3079	0.6603	0.7464	0.6382	0.8932	0.8617	0.6872	0.5769
6	0.6674	0.4443	0.667	0.7375	0.8418	0.8925	0.8617	0.6745	0.5615
7	0.6705	0.4493	0.6697	0.783	0.7327	0.8932	0.8463	0.5915	0.5
8	0.6953	0.4975	0.667	0.7813	0.7473	0.8938	0.8544	0.6085	0.4846
9	0.6829	0.1	0.6671	0.8027	0.74	0.8938	0.4727	0.3723	0.1
10	0.7016	0.517	0.6732	0.8384	0.74	0.8911	0.5012	0.7809	0.7
11	0.5744	0.5087	0.6762	0.8384	0.74	0.8966	0.5126	0.5553	0.5
12	0.5341	0.5216	0.6803	0.817	0.74	0.8897	0.5077	0.6383	0.5
13	0.4659	0.5287	0.6947	0.742	0.7473	0.8938	0.4866	0.6511	0.5769
14	0.4101	0.5615	0.7031	0.7393	0.7327	0.8952	0.4801	0.5489	0.5308
15	0.3388	0.3391	0.7019	0.858	0.7473	0.8979	0.5151	0.5532	0.6077
16	0.3977	0.4921	0.7044	0.8491	0.7327	0.8925	0.5069	0.5298	0.6231
17	0.3698	0.4879	0.7013	0.8241	0.74	0.8986	0.5216	0.4404	0.5462
18	0.345	0.5279	0.6983	0.7589	0.74	0.8932	0.5183	0.4851	0.5615
19	0.2364	0.7836	0.6979	0.7652	0.7473	0.8966	0.5321	0.5872	0.6077
20	0.2612	0.9	0.7994	0.783	0.74	0.9	0.7275	0.4851	0.5769
21	0.2333	0.8655	0.5228	0.7786	0.74	0.8891	0.7275	0.4255	0.5
22	0.1589	0.8364	0.4201	0.7732	0.74	0.8911	0.7405	0.4043	0.5308
23	0.1	0.8459	0.1	0.7616	0.7327	0.8891	0.738	0.3404	0.4077
24	0.3016	0.831	0.891	0.808	0.74	0.8973	0.7568	0.3553	0.5308
25	0.3822	0.799	0.8798	0.7179	0.74	0.165	0.7755	0.2723	0.4846
26	0.5124	0.6356	0.887	0.7196	0.74	0.1267	0.7779	0.3957	0.6692
27	0.5682	0.6447	0.8782	0.7429	0.74	0.1246	0.7706	0.5021	0.6692
28	0.5341	0.648	0.873	0.8125	0.74	0.1	0.7673	0.4	0.4692
29	0.4008	0.6405	0.874	0.7964	0.74	0.1281	0.7649	0.4702	0.5769
30	0.3729	0.6335	0.8752	0.7884	0.74	0.1376	0.7682	0.4362	0.4846
31	0.4039	0.6351	0.875	0.7518	0.74	0.1349	0.7682	0.4787	0.5462
32	0.4473	0.6193	0.8858	0.7089	0.7327	0.1308	0.7812	0.5511	0.5615
33	0.6023	0.6268	0.8836	0.742	0.7327	0.1171	0.7934	0.6915	0.7154
34	0.6519	0.6164	0.879	0.7375	0.4855	0.1486	0.808	0.583	0.6231
35	0.6457	0.6081	0.8786	0.7473	0.4709	0.7624	0.8105	0.266	0.1923
36	0.5868	0.6123	0.895	0.7875	0.5073	0.7501	0.7991	0.5979	0.6538
37	0.5961	0.621	0.9	0.7964	0.6745	0.7583	0.7934	0.4128	0.4231
38	0.5279	0.6243	0.8983	0.8045	0.9	0.7919	0.7787	0.3106	0.2846
39	0.5093	0.6202	0.8953	0.7375	0.7327	0.7837	0.7787	0.5894	0.6692
40	0.593	0.6277	0.8979	0.7402	0.74	0.7659	0.782	0.4	0.3923
41	0.5372	0.6314	0.8999	0.717	0.7473	0.7563	0.7755	0.5787	0.6846
42	0.5155	0.6459	0.8996	0.7732	0.7327	0.7467	0.7739	0.4468	0.5462
43	0.3233	0.6497	0.8942	0.7687	0.7109	0.7474	0.7885	0.5532	0.6077
44	0.2519	0.6979	0.7915	0.8027	0.3618	0.7419	0.8023	0.5128	0.5615
45	0.4473	0.6921	0.7851	0.8205	0.2455	0.7385	0.8162	0.6213	0.6231
46	0.5186	0.6946	0.7795	0.758	0.7691	0.7289	0.8202	0.7149	0.7154
47	0.5496	0.6846	0.7805	0.8161	0.74	0.7234	0.817	0.5489	0.5462
48	0.4814	0.7062	0.7815	0.8214	0.7473	0.7009	0.8113	0.6596	0.7308
49	0.4194	0.6888	0.7811	0.8616	0.7327	0.6933	0.8202	0.8	0.9
50	0.3636	0.6925	0.7843	0.883	0.74	0.7009	0.8072	0.5809	0.5462

predicted by the ICO-VSA-RNN model, while the curve marked with circles is the real MI value obtained from analysis in laboratory. Obviously, the results of training are good and almost all the points predicted by the ICO-VSA-RNN model match the real points.

The testing results are listed in Table I, which shows that the ICO-VSA-RNN model has the best performance on the testing dataset. It can be seen that RBF NN model gives an MAE of 0.0293, an MRE of 1.12%, a RMSE of 0.0409 and a TIC of 0.0078. For the ICO-VSA-RNN model, compose by a group of RBF NNs optimized with the ICO-VSA algorithm, has an MAE of 0.0078, an MRE of 0.30%, a RMSE of 0.0086 and a TIC of 0.0016. It shows that the ICO-VSA-RNN model has much better quality than the signal NN model. Compared with the RBF NN model the MAE, MRE, RMSE, and TIC are 0.0215, 0.82%, 0.0323, and 0.0062, with percentage decrease of 73.38%, 73.21%, 78.97%, and 79.49%,

respectively. These data prove that the ICO-VSA-RNN model provides wonderful MI prediction accuracy for the propylene polymerization process.

A visual way to show how much better the ICO-VSA-RNN model works than the RBF NN model do on the testing dataset is represented in Figure 3. The curve marked with crosses is the MI value predicted by the ICO-VSA-RNN model, while the curve marked with circles is the real MI value obtained from analysis in laboratory. The results predicted by RBF NN model are depicted by curves marked with asterisks. It shows that the result of the ICO-VSA-RNN model is better that the RBF NN model and nearly being the real MI value on most points. This visual comparison shows the high accuracy of the ICO-VSA-RNN model in the prediction of MI value.

To see more about the universality of the proposed MI prediction models, models are further evaluated on the generalization dataset. An accurate prediction of MI on this dataset gives a strong support that the proposed model owns good universality.

Table II shows the ICO-VSA-RNN model also has the best performance on the generalization dataset. It shows that the ICO-VSA-RNN model has much better quality than the signal RBF NN model. Compared with the RBF NN model the MAE, MRE, RMSE, and TIC are 0.0210, 0.79%, 0.0232, and 0.0044, with percentage decrease of 67.52%, 66.95%, 69.46%, and 69.84% respectively. It shows that the ICA-VSA-RNN model has a better universality than the RBF NN model.

However, another visual comparison to show two models work on generalization dataset is also shown in Figure 4. The curve marked with crosses is the MI value predicted by the ICO-VSA-RNN model, while the results predicted by RBF NN model are depicted by curves marked with asterisks. The curve marked with circles is the real MI value obtained from analysis in laboratory. Absolutely, the ICO-VSA-RNN model gives a nearly real MI value prediction, much more accurate than RBF NN model. After all, Table II and Figure 4 prove that the ICO-VSA-RNN model holds better universality in MI prediction both in data and graph.

Table III shows the comparison of the MI prediction results between our work and published literatures. Compared with the results of Shi and Liu,[14] Shi and Liu,[15] and Li and Liu[13] the MRE are 2.73%, 2.49%, and 0.83%, with percentage decrease of 88.97%, 87.95%, and 63.86%, respectively. It is clear that the results of our work are much better than those published works.

CONCLUSION

A method uses an optimized RBF neural network for PP MI prediction from other variables is presented in this article. The RBF neural network is optimized by an ICO-VSA algorithm, which added the ICO first and then combined the VSA to optimize the parameters of the RBF neural network at last. The proposed ICO-VSA-RNN model predicts MI with mean relative errors of 0.3% on the test dataset, compared with mean relative errors of 1.12% from RNN model. It obtains even smaller prediction error than the RNN model does, with a decrease percentage of 73.38% and 67.52% in MRE on testing dataset and generalization dataset respectively, compared with that of ICO-VSA-RNN model. The results reveal that the proposed model presents the relationship of the process variables and the target MI of the PP process successfully. And this intelligent model will be applied widely in the area for prediction of MI because of its wonderful performance.

NOMENCLATURE

MI	Melt index
PP	polypropylene
RBF	Radial basis function
CO	Chaos optimization
ICO	Improved chaos optimization
RNN	RBF neural network
VSA	Variable-scale analysis
PLS	Partial least squares
SVM	Support vector machines
PCA	Principal component analysis
PLS	Partial least squares
PSO	Particle swarm optimization
SA	Simulated annealing
ICA	Independent component analysis
MSA	Multi-scale analysis
LS	Least squares
CSTR	Continuous stirred-tank reactors
FBR	Fluidized-bed reactors
MAE	Mean absolute error
MRE	Mean relative error
RMSE	Root of mean square error
TIC	Theil's inequality coefficient
$\|\| \cdot \|\|$	The Euclidean distance
N	The number of the hidden layer nodes
$\Phi(\cdot)$	The result of the hidden layer node
w_{ki}	The output weight
x_p	The input vector
y_k	The output of its corresponding output node
M	The number of the output nodes
c_i	The center of its corresponding node in the hidden layer
σ_i	The width of its corresponding node in the hidden layer
x_i	The chaotic variable in the ICO-VSA-RNN hybrid algorithm
f_i	The corresponding target variable of x_i
a_i, b_i	The parameters of the VSA use to optimize x_i

x_i^* The chaotic variable that has been optimized by the VSA
t, m The optimization factors
w The parameters of the RNN model
best_w The best parameters of the RNN model
y_i, $\hat{y}_i$ The measured value and the predicted result of MI respectively

Reference

1. Jin, X. L.; Hu, P. H.; Yuan, P. Development of PP melt index inferential model, WCICA 2006. In Proceedings of the Sixth World Congress on Intelligent Control and Automation, 2006; Dalian, China: Institute of Electrical and Electronics Engineers Inc., Vol. 1, p 4866.
2. Bafna, S. S.; Beall, A. M. J Appl Polym Sci 1997, 65, 277.
3. McAuley, K. B.; MacGregor, J. F. AIChE J 1991, 37, 825.
4. Ahmad, S.; Mohamed, A. H.; Farouq, S. M.; Navid, M. Chem Eng J 2010, 161, 240.
5. Lee, E. H.; Kim, T. Y.; Yeo, Y. K. Korean J Chem Eng 2008, 25, 613.
6. Palmer, G.; Demarquette, N. R. Polymer 2005, 46, 8169.
7. Achilias, D. S.; Verros, G. D. J Appl Polym Sci 2010, 116, 1142.
8. Yuan, C.; Xinggao, L. Polymer 2005, 46, 9434–9442.
9. Lee, E. H.; Kim, T. Y.; Yeo, Y. K. Korea J Chem Eng 2008, 25, 613.
10. Ahmed, F.; Nazir, S.; Yeo, Y. K. Korea J Chem Eng 2009, 26, 14.
11. Han, I. S.; Han, C.; Chung, C. B. J Appl Polym Sci 2005, 95, 967.
12. Kong, W.; Yang, J. J Chem Ind Eng (China) 2003, 54, 1160 (in Chinese).
13. Li, J.; Liu, X. Neurocomputing 2010, 74, 735.
14. Shi, J.; Liu, X. G. Chin J Chem Eng 2005, 13, 849.
15. Shi, J.; Liu, X. G. J Appl Polym Sci 2006, 101, 285.
16. Shi, J.; Liu, X. G.; Sun, Y. X. Neurocomputing 2006, 70, 280.
17. Xu, Y. B.; Zheng, J. G. Intell Computing Inf Sci 2011, 134, 173.
18. Scarselli, F.; Tsoi, A. C. Neural Networks 1998, 11, 15.
19. Elanayar, S.; Shin, Y. C. IEEE Trans Neural Networks 1994, 5, 594.
20. Rivas, V. M.; Merelo, J. J.; Castillo, P. A.; Arenas, M. G.; Castellano, J. G. Inf Sci 2004, 165, 207.
21. Yu, D. L.; Gomm, J. B.; Williams, D. Control Eng Pract 1999, 7, 49.
22. Guo, Z.; Wang, S.; Zhuang, J. Pattern Recognit Lett 2006, 27, 2.
23. Senkerilk, R.; Davendra, D.; Zelinka, L. IEEE Congr Evol Comput 2010.
24. Gao, D.; Yang, G. Pattern Recognit 2003, 36, 869.
25. Chen, P.; Li, X.; Ren, S. B.; Li, W. H. Adv Mater Res 2011, 171, 555.
26. Marrero, J. M.; Garcia, A.; Linares, A. Nat Hazards Earth Syst Sci 2010, 10, 747.
27. Luo, Y.; Tang, G.; Zhou, L. Appl Soft Comput 2008, 8, 1068.
28. Yang, D.; Li, G.; Cheng, G. Chaos Solitons Fractals 2007, 34, 1366.
29. Mohammad, S. T.; Mohammad, H. Appl Math Comput 2007, 187, 1076.
30. Wang, H. N.; Sun, S.Q.; Wu, J. F. Smart Mater Intell Syst 2011, 143, 1280.
31. Song, Y.; Chen, Z.; Yuan, Z. Chin J Chem Eng 2007, 15, 539.
32. Rani, M.; Agarwal, R. Chaos Solitons Fractals 2009, 42, 447.
33. Rani, M.; Agarwal, R. Chaos Solitons Fractals 2009, 41, 2062.
34. Murray-Smith, D. J. Math Compt Model Dyn Syst 1998, 4, 5.